

Microstructure-Property Relations of Hot-Pressed Silicon Carbide-Aluminum Nitride Compositions at Room and Elevated Temperatures

Ahmad H. Lubis,[†] Norman L. Hecht, and George A. Graves Jr.*

University of Dayton Research Institute, University of Dayton, Dayton, Ohio 45469-0172

Robert Ruh*

Universal Technology Corporation, Beavercreek, Ohio 45432-2600

A series of SiC-AlN compositions of 0, 10, 25, 50, 75, 90, and 100 mol% AlN were hot pressed at 2100°C for a 1 h soak at a pressure of 35 MPa under vacuum. 2H-wurtzite SiC-AlN solid-solution structures were formed for compositions with 25–100 mol% AlN. The associated lattice parameters for these solid solutions followed Vegard's law. The microstructures varied with composition; the number of needlelike grains decreased for compositions up to 25 mol% AlN and the amount of equiaxed grains increased for compositions with 25–100 mol% AlN. Densities for all the specimens were >99% of the theoretical density. Coefficients of thermal expansion varied from $4.80 \times 10^{-6}/^{\circ}\text{C}$ to $6.25 \times 10^{-6}/^{\circ}\text{C}$ in the 20°–1400°C range. Young's moduli varied from 451 GPa to 320 GPa at room temperature (RT) and retained 98%, 96%, and 94% of their RT values at 500°, 1000°, and 1250°C, respectively. These three properties correlated linearly with composition. RT microhardness varied from 21.6 GPa to 11.2 GPa and correlated linearly with composition within the solid-solution range. Flexural strengths increased from 487 MPa to 604 MPa from 0 mol% AlN to 25 mol% AlN and then decreased to 284 MPa for 100 mol% AlN. At 1250°C, flexural strengths decreased from 90% to 65% of the RT values. Fracture toughness increased from 3.6 MPa·m^{1/2} to 4.2 MPa·m^{1/2} from 0 mol% AlN to 10 mol% AlN and then decreased to 2.5 MPa·m^{1/2} for 100 mol% AlN.

I. Introduction

SILICON CARBIDE (SiC) and aluminum nitride (AlN) are prominent materials that are used in various high-temperature (HT) and electrical applications. SiC is a covalent compound and can occur in either β -SiC or α -SiC crystal structures.^{1,2} Both α -SiC and AlN are covalent hexagonal with 2H-wurtzite crystal structures and are classified in the *P63mc* space group.³ SiC has good oxidation and corrosion resistance, relatively high thermal conductivity, and good mechanical properties, and it is classified as a semiconductor material.^{2,4,5} AlN has high thermal conductivity, high electrical resistivity, and good chemical resistance, which makes it a leading ceramic material for refractory and substrate applications.^{4,6} However,

AlN has only moderate microhardness and flexural strength.^{5,7} The phase diagram for the alloys of SiC and AlN shows a 2H-wurtzite solid-solution series at high temperature in the composition range of 25–100 mol% AlN. Several studies on alloying the two materials for different applications have been reported.^{1,5,8–14} Many of these studies have investigated the processing variables and property values for many SiC-AlN alloys, and a summary has been given by Lubis.¹⁵ However, a more detailed and systematic correlation of composition versus properties must be established.

A comprehensive study to investigate a range of alloy compositions and the role of HT thermal treatments was initiated. The objective of this work was twofold: (i) to fabricate a series of 2H-wurtzite SiC-AlN solid-solution compositions via hot pressing and to investigate the reproducibility of phases, microstructures, and their corresponding properties; and (ii) to serve as a basis to study the methodology for fabricating and characterizing nanophased reinforced composites from the SiC-AlN system via heat treatment within the spinodal decomposition zone. The work performed in the first part of the objective was intended to provide a more complete database for the SiC-AlN system. The results of the second part of the objective will be reported in a subsequent paper.

II. Experimental Procedure

(1) Sample Fabrication

The SiC-AlN system was studied using compositions of β -SiC (Grade B10, cubic phase, H. C. Starck, Goslar, Germany) and AlN (Grade B, hexagonal phase, H. C. Starck). The as-received β -SiC had a particle size of 0.6 μm , Brunauer-Emmett-Teller (BET) surface area of 16 m²/g, and contained ≈ 95 wt% β -SiC and ≈ 0.1 wt% free silicon. Additional chemical elements included 0.82 wt% of oxygen, 200 ppm of iron, 80 ppm of aluminum, and 6 ppm of calcium. In this study, β -SiC was doped with 2000 ppm of boron from boron carbide and 1 wt% of free carbon from a phenolic resin. The as-received AlN had a particle size of 1.0–2.5 μm , a BET surface area of 3.0–6.0 m²/g, and was single-phase hexagonal. Additional chemical elements included 2.0 wt% of oxygen, 0.1 wt% of carbon, 0.005 wt% of iron, and 0.01 wt% of other metallic impurities. The above data were provided by the vendor.

Monolithic ceramic specimens of β -SiC, AlN, and five alloys from the SiC/AlN system (10, 25, 50, 75, and 90 mol% AlN) were prepared for this study via hot pressing. All the blends were dry ball-milled for 72 h and densified in a two-stage process. The powder blend first was cold pressed at 14 MPa and then hot pressed using graphite dies. As the firing temperature approached the recrystallization temperature ($\approx 1700^{\circ}\text{C}$), the pressure was increased to 35 MPa. Then, the temperature was increased to 2100°C and maintained for ≈ 60

L. C. DeLonghe—contributing editor

Manuscript No. 190262. Received April 10, 1998; approved January 15, 1999.

Supported by the General Electric Company.

*Member, American Ceramic Society.

[†]Now with Agency for the Assessment and Application of Technology, Jakarta 10340, Indonesia.

min. The hot-pressed (HP) system was cooled slowly to 900°C and then allowed to cool naturally. The specimens were 38 mm in diameter and 20 mm in height.

HP disks were prepared in three separate series of runs that were conducted at three different times during the course of the project. The disks were designated as batches 1, 2, and 3, depending on the time of fabrication. Test specimens for analysis were cut from the disks. The processing variables for each batch are identified in Table I.

As shown in Table I, although the processing conditions varied, almost all the samples were hot pressed at ~2100°C. The specimens obtained from batches 1, 2, and 3 were used to measure density, hardness, fracture toughness, and room temperature (RT) flexural strength. The specimens from batch 3 were used to measure the flexural strength at 1250°C, and those from batch 1 were used to measure the coefficient of thermal expansion (CTE) up to 1400°C. A more detailed description of the sample-fabrication procedures and testing protocol has been presented by Lubis.¹⁵

(2) Ceramographic Techniques

Diamond-saw sectioning was followed by use of an automatic grinding/polishing machine. Mounting was performed using a mixture of epoxy resin (Epofix Resin, Struer, Westlake, OH) and hardener (triethylene tetramine) in a ratio of 15:2. This type of mounting procedure avoids the generation of pressures that may produce cracks or other damage to the specimen. The grinding and polishing details have been described elsewhere.¹⁵ Etching of the polished specimens was achieved using boiling Murakami's reagent (10 g of KOH, 10 g of $K_2Fe(CN)_6$, and 100 mL of distilled water).¹⁶ Microstructural analyses were conducted using both optical microscopy and scanning electron microscopy (SEM). For the SEM and energy-dispersive X-ray (EDX) work, the SiC-AIN specimens were sputter coated with carbon in a vacuum evaporator chamber.

(3) Phase Analyses and Lattice Parameter Determinations

Specimens cut from the HIP billets were analyzed using a $CuK\alpha$ target with X-ray radiation with an average wavelength of 1.54059 Å. The X-ray studies were conducted at 2 θ values in the range of 10°–150° at a scanning speed of 1°/20/min for both phase and lattice parameter determinations. The lattice parameters were calculated using the least-squares method.

(4) Structural and Physical Properties Determination

Density was determined using the ASTM C 693-84 standard test method,² and the crystallographic density was calculated based on the fractional weight of SiC and AIN over the unit-cell volume. The unit-cell volume was calculated from the lattice parameters a and c . Knoop microhardness measurements were made at room temperature, following the ASTM C 849-88 standard test method (Automated Micromet 2004 Knoop Microhardness Tester, Buehler, Lake Bluff, IL), using

loads of 500 g for all compositions. CTE values were measured twice using a double push-pull rod dilatometer (Dilatronic II, Model 6024, Theta Industries, Port Washington, NY) that was equipped with an automatic recording system; the CTE measurements were based on the ASTM E 228-71 test standard. The CTE was measured from room temperature to 1400°C, using a heating rate of 200°C/h under vacuum (~4 kPa (30 torr)). The specimens used were 25.4 mm × 3.0 mm × 4.0 mm, and both ends were ground parallel to guarantee good contact and prevent misalignment. A platinum specimen was used as a reference standard to calculate the CTE values. The Young's and shear moduli were measured using an impulse vibration technique (Grindosonic Model MR3ST, J. W. Lemmens, St. Louis, MO), based on the ASTM C 1259-94 test method. In this study, a disk specimen 38.1 mm in diameter and 2 mm thick was used. The measurements were conducted at temperatures of 20°, 500°, 1000°, and 1250°C in air. Fracture toughness values were determined using the empirical indentation technique that was developed by Evans and Charles.¹⁷ Four-point flexural strengths were determined using a modification of the ASTM C 1161-90 test method for RT tests and the ASTM C 1211-92 test method for HT tests. The dimensions of the flexure specimens were 25.4 mm × 3.0 mm × 4.0 mm. The edges were chamfered to avoid sharp edges that could act as stress concentrators. Both RT and HT flexural tests were conducted in air. A crosshead speed of 0.254 mm/min was selected for all the measurements. Stainless-steel and SiC fixtures, with upper and lower spans of 20.0 and 10.0 mm, respectively, were used for the RT and HT tests. The RT and HT flexural tests were conducted in a testing machine (Model 55R1123, Instron Corp., Canton, MA).

III. Results and Discussion

(1) Characterization of As-Received SiC and AIN Powders

Both the β -SiC and AIN particles were approximately spherical; their average particle sizes were 0.7 and 1.8 μ m, respectively (Fisher Sub Sieve Sizer (FSSS), Fisher Scientific, Pittsburgh, PA). The measured BET surface areas of the β -SiC and AIN were 14 and 3 m²/g, respectively. The results were comparable with data provided by the vendor. Trace levels of aluminum, oxygen, magnesium, sodium, nitrogen, and fluorine impurities were detected in the SiC; oxygen, magnesium, sodium, and fluorine impurities were detected in the AIN. No iron or calcium, which was reported to be present by the manufacturer, was detected.

X-ray diffraction (XRD) patterns identified the β -cubic phase for SiC and the 2H hexagonal phase for AIN. The calculated lattice parameter a for cubic β -SiC was 4.3600 ± 0.0002 Å, and lattice parameters a and c for AIN were 3.1118 ± 0.0002 Å and 4.9806 ± 0.0002 Å, respectively. These results are in good agreement with the literature data for a for β -SiC (4.3589 Å) and a and c for AIN (3.1114 and 4.9792 Å, respectively).³

The sodium and fluorine in both the SiC and the AIN powders (and nitrogen in the SiC powder) probably was introduced

Table I. Hot-Pressing Conditions for Batches 1, 2, and 3^a

SiC-AIN specimens (mol% AIN)	Preparation conditions, Batch 1			Preparation conditions, Batch 2			Preparation conditions, Batch 3		
	Hot-pressing temperature (°C)	Heating rate (°C/h)	Cooling rate (°C/h)	Hot-pressing temperature (°C)	Heating rate (°C/h)	Cooling rate (°C/h)	Hot-pressing temperature (°C)	Heating rate (°C/h)	Cooling rate (°C/h)
0	2066	2045	772	2104	1205	905			
10	2113	1142	603	2116	1571	1246	2100	624	1900
25	1937	884	693	2100	1387	1275	2100	600	1165
50	2070	1025	954				2100	570	1390
75	2070	1025	954	2080	633	1030	2080	560	1370
90	2050	870	765	2080	620	1000	2080	560	1380
100	2070	1025	954	2910	1260	1325			

^aThe SiC-AIN specimens were hot-pressed at a pressure of 35 MPa for a soaking time of 1 h under vacuum.

during material synthesis and processing. Under HT processing, sodium and fluorine may not be detrimental, because these elements or their compounds probably volatilize. The presence of >0.1 wt% of impurities can inhibit the formation of a solid solution, because of the formation of separate phases. For instance, the presence of iron can stabilize β -SiC.^{8,18}

(2) Microstructural Analyses of the Hot-Pressed SiC-AIN System

The microstructures of the HP SiC-AIN system were dependent on composition. However, other factors such as the consolidation methodology, temperature, soaking time, time-temperature cycle, pressure, and atmosphere also can affect the microstructures. The microstructures obtained for the 0%, 10%, 25%, 50%, 75%, 90%, and 100% SiC compositions, both

perpendicular and parallel to the hot-pressing directions, are presented in Figs. 1 and 2.

The 100% SiC specimens that were hot pressed in two separate batches had almost identical microstructures: randomly oriented, large needlelike grains of various grain sizes (2–2.5 μm) and aspect ratios (4–5), as shown in Fig. 1. A platelike structure also was observed.¹⁶

The microstructure for the SiC-10 mol% AIN specimens was composed of randomly oriented, needlelike grains that were accompanied by a small percentage of equiaxed grains. The grain sizes varied over a range of 5–20 μm and the aspect ratios varied over a range of 6–7; both ranges were higher than those of the 100% SiC, because of the needlelike grains. Few pull-out grains were observed.

For the SiC-25 mol% AIN (Fig. 1), the microstructure

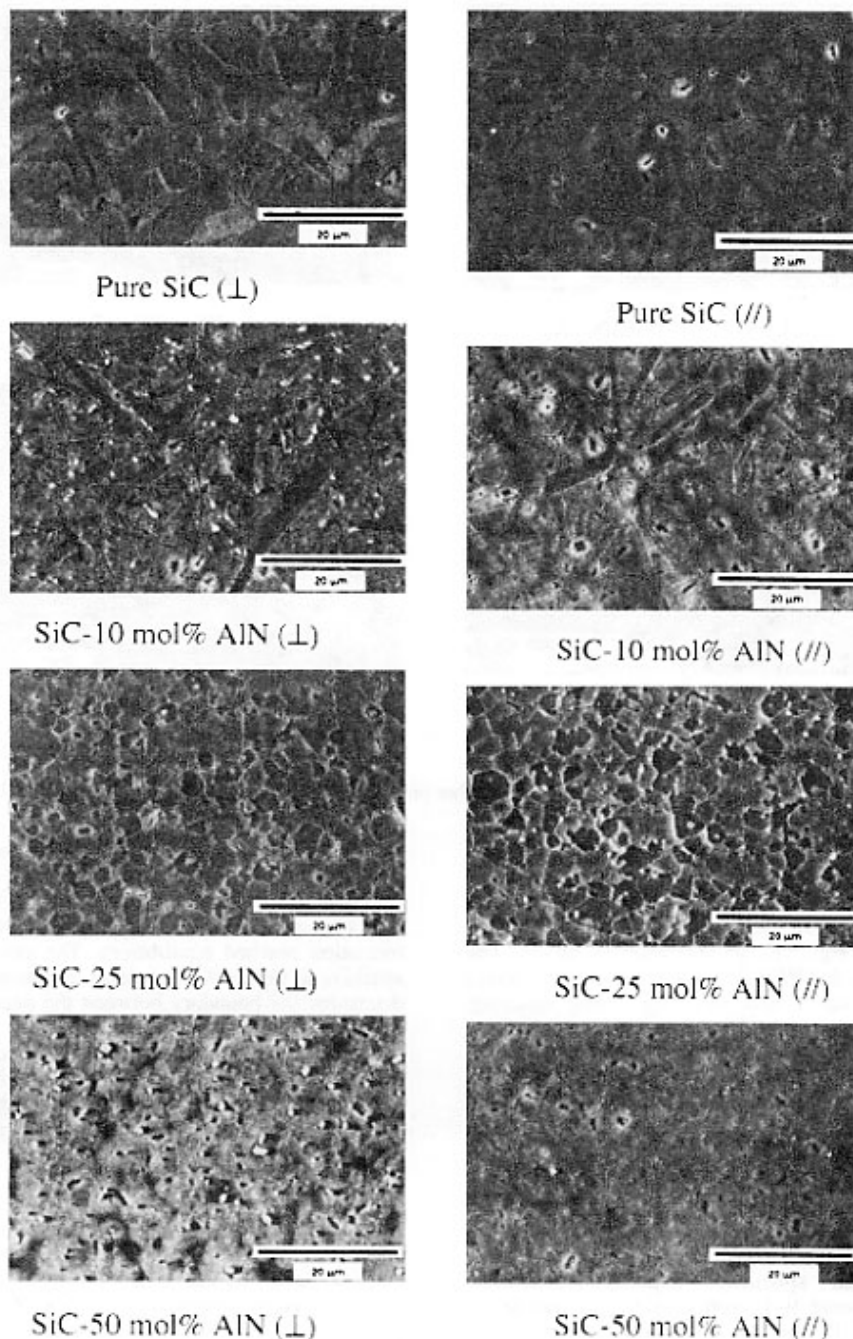


Fig. 1. SEM micrographs of representative microstructures of the hot-pressed SiC-AIN specimens (AIN contents of 0, 10, 25, and 50 mol%). Bar = 20 μm .

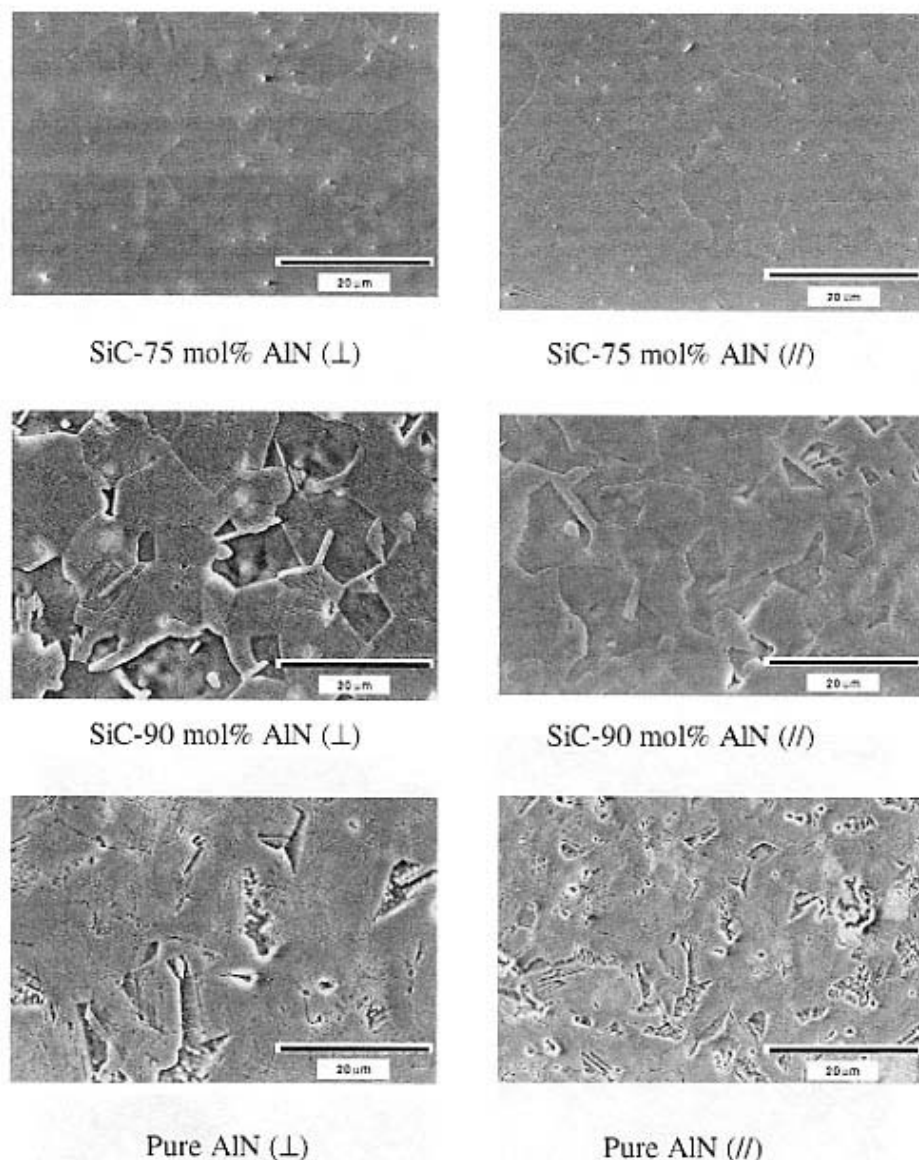


Fig. 2. SEM micrographs of representative microstructures of the hot-pressed SiC-AlN specimens (AlN contents of 75, 90, and 100 mol%). Bar = 20 μm .

changed from a needlelike structure to an equiaxed grain structure of $\sim 3 \mu\text{m}$ grains that were accompanied by a very small percentage of elongated grains. The minimum amount of AlN, for the formation of equiaxed grains, was 25 mol%. The specimens with 25 mol% AlN had an equiaxed grain structure without significant grain growth occurring during sintering. The role of boron, in this case, was not as effective as that observed for compositions with higher SiC contents (< 25 mol% AlN).

For the SiC-AlN compositions with > 25 mol% AlN, the microstructures remained equiaxed as the grain size increased. The SiC-50 mol% AlN specimens (Fig. 1) consisted of equiaxed grains 3–6 μm in size, depending on the hot-pressing conditions. Few pores were observed within the grains or at the triple points. The SiC-75 mol% AlN specimens (Fig. 2) showed equiaxed grains 8–11 μm in size and some pullouts. The SiC-90 mol% AlN specimens (Fig. 2) also showed equiaxed grains that were 9–15 μm in size and had fewer pores. The HP 100% AlN specimens showed equiaxed grains with faulted and strained grains.

As reported, the formation of the solid solution was initiated after the 3C-SiC transformed to 2H-SiC.⁵ A diffusion couple

study suggested that SiC diffuses more easily into AlN than AlN into SiC.¹⁹ At compositions of > 25 mol% AlN, the SiC-AlN system sintered to a higher density after the solid-solution formation reached equilibrium. The grain growth was quite sensitive to higher AlN contents. In general, it was difficult to determine the boundary between the needlelike and equiaxed grains.

The light and dark areas in the SEM micrographs may be due to grain orientation.^{16,20–22} The SiC-AlN compositions with higher AlN content seem to exhibit more-uniform color. This observation suggests that greater AlN content will give more-uniform grain orientation.

(3) Phase Identification

XRD spectra showed that the 2H-wurtzite structure was predominant in specimens with ≥ 25 mol% AlN. The X-ray analyses indicated the presence of 2H, 4H, 6H, and 15R phases in the SiC and SiC-10 mol% AlN. The 25 and 50 mol% AlN specimens contained trace amounts of 4H and 15R phases. The 75, 90, and 100 mol% AlN specimens contained only the 2H-wurtzite structure.

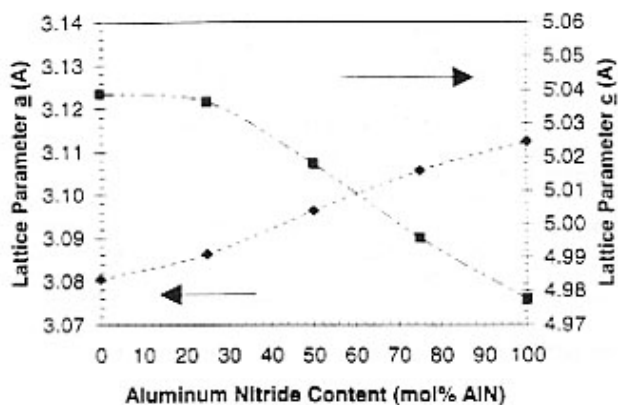


Fig. 3. Lattice parameters *a* and *c* of the hot-pressed SiC-AlN specimens.

(4) Lattice Parameter Determinations

Despite the presence of other phases, the 2H lattice parameters of HP SiC could be calculated by refining the 2H peaks. The lattice parameters *a* and *c* increased and decreased, respectively, as the AlN content increased following Vegard's law, starting from 25 mol% AlN, as shown in Fig. 3. This observation indicates that these compositions undergo complete solid-solution formation.

(5) Physical and Structural Properties and Correlation with Microstructure

(A) *Density*: The densities of the majority of HP SiC, AlN, and SiC-AlN specimens were >99% of the theoretical density and approached crystallographic densities. Batch-to-batch variation was small (<1%). Figure 4 illustrates the linear correlation of density with composition, especially in the 25–90 mol% AlN region. As suggested by other investigators,^{1,2,3–26} the use of hot pressing and the addition of boron and free carbon resulted in high-density SiC-AlN specimens. These results are in good agreement with the values that have been reported in the literature.

(B) *Coefficient of Thermal Expansion*: The average CTE values of the SiC-AlN specimens, measured from room temperature to 1400°C, increased as the AlN content and temperature increased (Fig. 5). The results suggest that the SiC-AlN compositions were relatively stable up to 1400°C, with no indication of phase change. The CTE results were consistent with the lower melting point and lower degree of covalent bonding of AlN, compared with that of SiC, and agreed with reported values.^{4,5,8}

(C) *Young's and Shear Moduli and Poisson's Ratios*: The measured RT Young's modulus and shear modulus, and the calculated Poisson's ratio results at 20°C, are presented in Fig. 6. As expected, the Young's and shear moduli decrease linearly as the AlN content increases. The results were similar to the literature values.^{8,23} The Young's and shear moduli of the SiC-AlN specimens that were measured at 500°, 1000°,

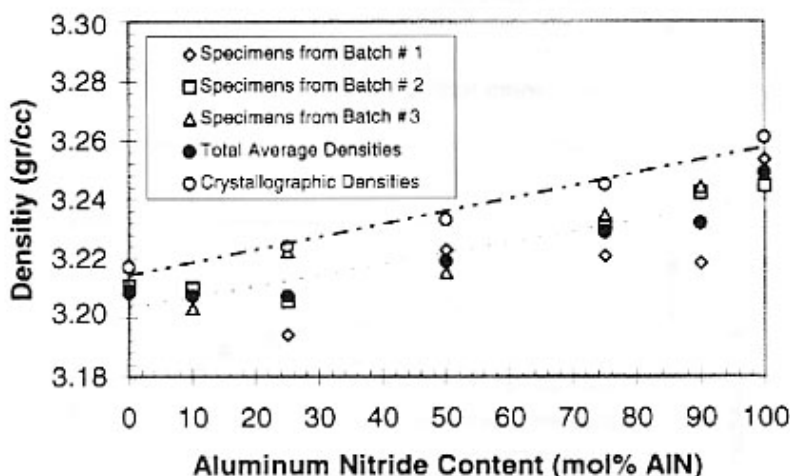


Fig. 4. Density values of the hot-pressed SiC-AlN specimens for different compositions.

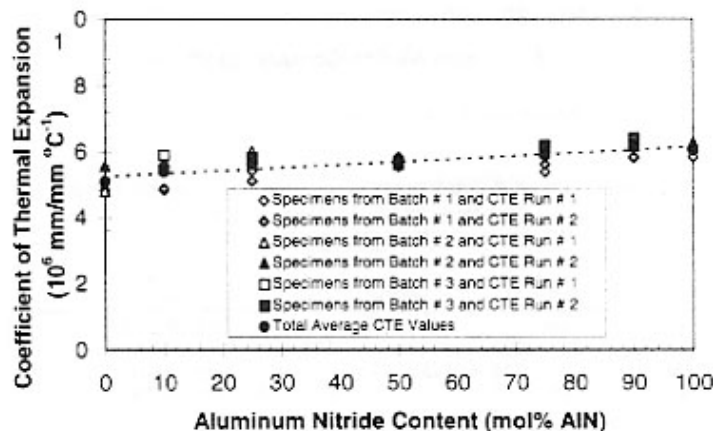


Fig. 5. Average CTE values of the hot-pressed SiC-AlN specimens, measured from room temperature to 1400°C.

and 1250°C decreased as the temperature increased. The associated Poisson's ratios increased as the AlN content increased (Fig. 6); however, the temperature effect was small. Experimental data were corrected for porosity, using the results from Ruh et al.²³

(D) *Knoop Microhardness*: Figure 7 shows that the Knoop microhardness values decrease almost linearly as the AlN content increases for the entire compositional region. This trend and the hardness values obtained are in good agreement with the values that were reported by Ruh and Zangvil.¹ The latter data are included in Fig. 7. The standard deviation for each specimen was <4%, which implies that the specimens have a high degree of uniformity. The agreement also was relatively good from batch to batch.

(E) *Flexural Strength*: A summary of the RT flexural strength measurements for the SiC–AlN test specimens from batches 1, 2, and 3 is presented in Table II. The average RT flexural strengths for the SiC-rich region increase to a maximum at 25 mol% AlN and then decrease as the AlN content increases. As shown in Figs. 1 and 2, the microstructure changes from needlelike grains to equiaxed grains in the 0–25 mol% AlN region. The SiC–25 mol% AlN specimen has the finest equiaxed grain size, compared to the other compositions that have been investigated. The increase in average flexural strength, up to 25 mol% AlN, is attributed to grain-size reduction. The microstructures for the specimens with >25 mol% AlN are equiaxed but have increasing grain size with increasing AlN content and decreasing average flexural strengths, as

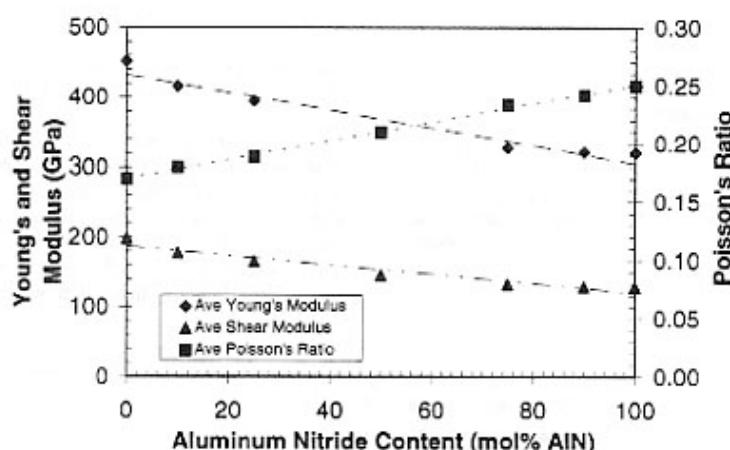


Fig. 6. Room temperature Young's and shear moduli, and the Poisson's ratio, of SiC, AlN, and the SiC–AlN compositions.

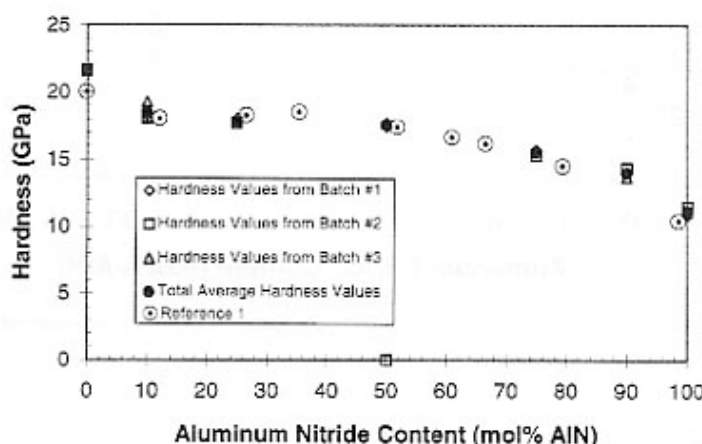


Fig. 7. Room temperature Knoop microhardness values of the selected hot-pressed SiC–AlN specimens.

Table II. Summary of Room Temperature Flexural Strength Results for the Hot-Pressed SiC–AlN Specimens

SiC–AlN specimen (mol% AlN)	Flexural strengths (MPa)			Average value and standard deviation	Coefficient of variance (%)
	Batch 1	Batch 2	Batch 3		
0	466, 419	590, 474		487.25 ± 72.7	15
10	613, 595	474, 497	467, 564	535 ± 76.4	14
25	714, 725	462, 567	513, 640	603.5 ± 107.56	18
50	425, 507		620, 646	549.5 ± 102.61	19
75	443, 331, 307	292, 279	358, 396	343.7 ± 59.4	17
90	260, 262	317, 346	258, 301	290.7 ± 36.58	13
100	304, 274	259, 297		283.5 ± 20.76	7

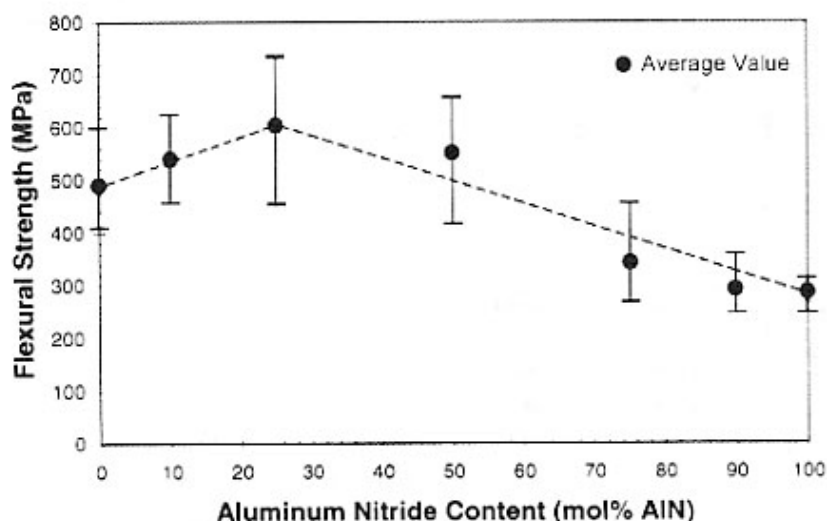


Fig. 8. Room temperature flexural strength values of the hot-pressed SiC-AIN specimens.

shown in Fig. 8. Several factors that affect the measured strengths may be related to the SiC:AlN ratio,^{1,14,26,27} grain-size reduction,^{1,5,14,27-29} and the interactions between SiC and AlN, such as interfacial bonding.^{14,29}

The obtained average RT flexural strength values were in reasonable agreement with the values reported in a review of literature data¹⁵ and followed the same general correlations between strength and composition. Although the deviation between and within batches was higher than expected, based on the small variances in the other property values, the range of values was within the reported variances of the literature data.¹⁵ Table II shows that the coefficient of variances were 7%–19% for the different compositions that have been investigated. This magnitude of batch-to-batch differences in flexural strength could not be explained readily.

The flexural strengths at 1250°C were measured on specimens taken from batch 3. The measured strength decreased as the AlN content increased, as shown in Fig. 9. The use of specimens from batch 3 provided valid comparisons between RT and HT flexural strength values versus composition. The flexural strength at 1250°C follows the same trend as that observed at room temperature. The flexural strengths at

1250°C are ~80% of the RT values for SiC-25 mol% AlN and ~65% for SiC-50 mol% AlN; however, for SiC-75 mol% AlN and SiC-90 mol% AlN, the values are ~90% of the RT strengths. It is suspected that, at high temperature, a flaw-healing effect may contribute to the strengthening, as reported by Li *et al.*²⁷

(F) *Fracture Toughness:* The trend for the RT fracture toughness values measured for the SiC-AIN specimens of different compositions are summarized in Fig. 10. The fracture toughness results were measured only for the values where the ratio of the half-crack length divided by half of the indent was >2.5. Fracture toughness values increased slightly up to 10 mol% AlN and then decreased slightly as the AlN content increased. The increase in fracture toughness up to 10 mol% AlN was attributed to the presence of needlelike grains in the microstructure. The microstructure changed from needlelike grains at 10 mol% AlN to equiaxed grains as the AlN content increased up to 25 mol%. The decrease in fracture toughness for specimens with ≥ 25 mol% AlN was attributed to the increasing grain size of the equiaxed grains and the intrinsic nature of both materials. The average fracture toughness values measured for the different SiC-AIN compositions were in good

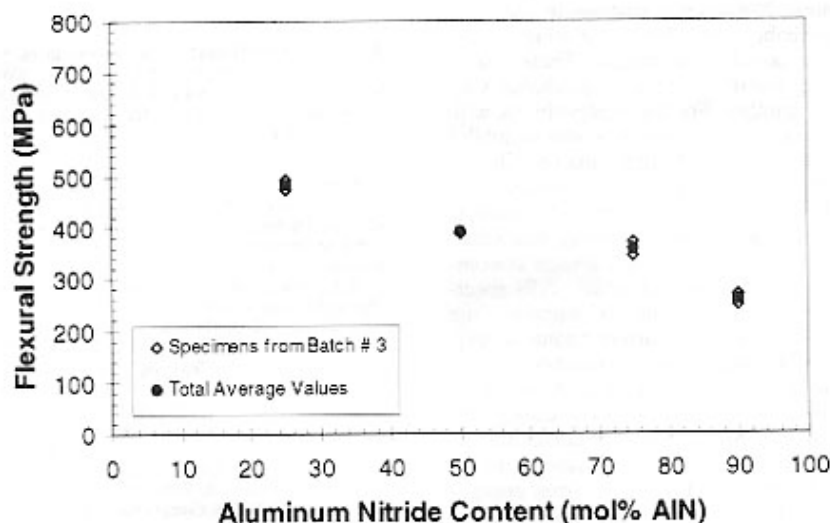


Fig. 9. Flexural strength values at 1250°C of the hot-pressed SiC-AIN specimens.

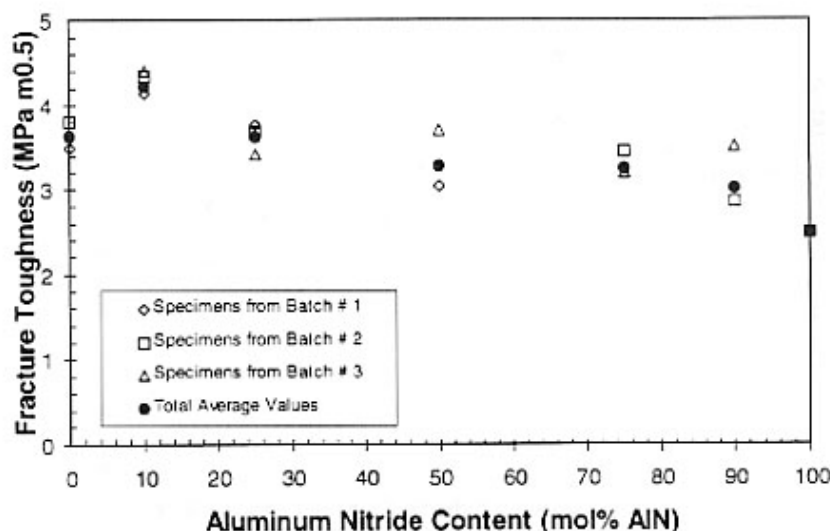


Fig. 10. Room temperature fracture toughness values of the hot-pressed SiC-AlN specimens.

agreement with the reported values and displayed little batch-to-batch variance.¹⁵ Overall, the fracture toughness values were not significantly different and were consistent with the results of other investigators.^{8,11,24,27,30} The behavioral trend of the fracture toughness relates to the microstructures that have been obtained for the different compositions.

IV. Summary and Conclusions

This work was designed to provide a more detailed and systematic investigation of the correlations between chemical composition, microstructure, and the thermal mechanical behavior of compounds in the silicon carbide-aluminum nitride (SiC-AlN) system. The results provide a more comprehensive picture of the SiC-AlN system and a basis for selecting the compositions for heat treatment below the spinodal temperature.

The morphologies of the hot-pressed (HP) SiC-AlN compounds were very dependent on composition. The amount of needlelike structures found at the SiC end decreased as the AlN content increased and were not visible as the AlN content approached 25 mol%. SiC-AlN compositions with ≥ 25 mol% AlN had an equiaxed grain structure and increasing grain size with increasing AlN content. Noticeable variations in grain size were observed, which probably were due to variations of the hot-pressing parameters, especially temperature. These results suggest that the free-energy minimization and equilibrium vary from one composition to another. For the compositions with needlelike grains, the effect of boron and AlN was to inhibit grain growth. For the case of equiaxed grains, the equilibrium state of the constituents is more compatible. It is suspected that the presence of AlN, boron, and carbon (each of which is dependent on composition) affects the free-energy minimization of all the SiC-AlN compositions. In fact, greater concentrations of boron and carbon are expected in SiC-AlN specimens in the SiC-rich area. It is difficult to determine the optimum amount of AlN, boron, and carbon quantitatively; however, the 25 mol% AlN composition is considered to be almost optimum, because it attained the finest grain structure.

The HP conditions used were effective in producing 2H-wurtzite solid solutions of ≥ 25 mol% AlN. The lattice parameters of the specimens prepared in this compositional range followed Vegard's law. In addition, the results from energy-dispersive X-ray analysis showed that the SiC-AlN system maintained its chemical stability at high temperature.

For the HP SiC-AlN specimens, the density and coefficient

of thermal expansion increased linearly as the AlN content increased and the Young's modulus decreased linearly as the AlN content increased. The room temperature (RT) Knoop microhardness decreased linearly as the AlN content increased, especially for specimens in the solid-solution region. For the SiC-AlN compositions with < 25 mol% AlN, Knoop microhardness values deviated from linearity, probably because of the presence of polytypic phases. RT four-point flexural strengths increased for compositions up to 25 mol% AlN, and fracture toughness values increased up to 10 mol% AlN. Beyond these AlN levels, the flexural strength and fracture toughness decreased. This result is believed to be due to the microstructures and the intrinsic bonding qualities of the SiC-AlN specimens. The Young's modulus, shear modulus, and Poisson's ratios decreased slightly as the temperature increased (RT Young's moduli values decreased 5% at 1250°C). Flexural strengths at 1250°C decreased for all compositions; however, for the 50 and 75 mol% AlN compositions, the decrease was only 10%. These results suggest that the SiC-AlN system can be used in moderate temperature and strength applications. The results also suggest the possibility of developing SiC-AlN layered composites, because of the linearity of the physical and thermal properties with composition within the solid-solution region.

Acknowledgments: The authors thank Steve Goodrich, Dale Grant, Stan Hilton, Doug Wolf, and Larry Sqrow (University of Dayton Research Institute, Dayton, OH) for their laboratory support. The authors also thank Dr. Ron Kerans, Dr. Paul Jero, Lawrence Matson, and Ms. Luanne Piazza (Wright-Patterson Air Force Base, OH) for their laboratory support.

References

- R. Ruh and A. Zangvil, "Composition and Properties of Hot Pressed SiC-AlN Solid Solutions," *J. Am. Ceram. Soc.*, **65** [5] 260-65 (1982).
- M. M. Dobson, "Silicon Carbide Alloys," pp. 1-132 in *Research Reports in Materials Science*, Series One, Edited by P. E. Evans, Parthenon, U.K., 1986.
- R. C. Evans, *An Introduction to Crystal Chemistry*, 2nd Ed. Cambridge University Press, London, U.K., 1966.
- G. Ervin, "Silicon Carbide-Aluminum Nitride Refractory Composite," U.S. Pat. No. 3 492 153, North American Rockwell Corp., Jan. 27, 1970.
- M. Landon and F. Thevenot, "The SiC-AlN System: Influence of Elaboration Routes on the Solid Solution Formation and Its Mechanical Properties," *Ceram. Int.*, **17** [2] 97-110 (1991).
- M. T. Cross, "Aluminum Nitride-Silicon Carbide Whisker Composites: Processing, Properties, and Microstructural Stability"; Master's Thesis, University of Illinois at Urbana-Champaign, Urbana, IL, 1990.
- K. S. Mazlouzas, R. Ruh, and E. E. Hermes, "Phase Characterization and Properties of AlN-BN Composites," *Am. Ceram. Soc. Bull.*, **64** [8] 1149-54 (1985).
- W. Rafanelli, K. Cho, and A. V. Virkar, "Fabrication and Characterization of SiC-AlN Alloys," *J. Mater. Sci.*, **16** [12] 3479-88 (1981).

- ⁹Y. Xu, A. Zangvil, and R. Ruh, "Formation of β -SiAlON as an Intermediate Oxidation Product of SiC-AIN Ceramics," *J. Am. Ceram. Soc.*, **78** [10] 2753-62 (1995).
- ¹⁰R. J. Osof, P. Korgul, and D. P. Thompson, "Fabrication of Aluminum Silicon Carbides"; presented at the 91st Annual Meeting of the American Ceramic Society, Indianapolis, IN, April 1989 (Paper No. 53-C-89).
- ¹¹W. Rafaniello, M. R. Plichta, and A. V. Virkar, "Investigation of Phase Stability in the System SiC-AIN," *J. Am. Ceram. Soc.*, **66** [4] 272-76 (1983).
- ¹²Z. C. Jou, S. Y. Kuo, and A. V. Virkar, "High Temperature Creep in Polycrystalline AlN-SiC Ceramics," *J. Mater. Sci.*, **21** [9] 3015-18 (1986).
- ¹³Z. C. Jou, S. Y. Kuo, and A. V. Virkar, "Elevated Temperature Creep of Silicon Carbide-Aluminum Nitride Ceramics: Role of Grain Size," *J. Am. Ceram. Soc.*, **69** [11] C-279-C-281 (1986).
- ¹⁴Y. Xu, A. Zangvil, M. Landon, and F. Thevenot, "Microstructure and Mechanical Properties of Hot-Pressed Silicon Carbide-Aluminum Nitride Composites," *J. Am. Ceram. Soc.*, **75** [2] 325-33 (1992).
- ¹⁵A. H. Lubis, "Development of a Methodology for Fabrication and Characterization of Nanophased Reinforced Composites from the Silicon Carbide-Aluminum Nitride System"; Ph.D. Dissertation, Materials Engineering Department, The University of Dayton, Dayton, OH, Dec. 1997.
- ¹⁶C. A. Johnson and S. Prochazka, "Microstructures of Sintered SiC"; pp. 366-77 in *Ceramic Microstructures '76*, Edited by R. M. Fulrath and J. H. Pask, Westview Press, Boulder, CO, 1977.
- ¹⁷A. G. Evans and E. A. Charles, "Fracture Toughness Determinations by Indentation," *J. Am. Ceram. Soc.*, **59** [7-8] 371-27 (1976).
- ¹⁸I. B. Cutler and P. D. Miller, "Solid Solution and Process for Producing a Solid Solution," US Pat. No. 414 174 027, University of Utah, Salt Lake City, UT, Feb. 27, 1979.
- ¹⁹A. Zangvil and R. Ruh, "Solid Solutions and Composites in the SiC-AIN and SiC-BN System," *Mater. Sci. Eng.*, **71**, 159-64 (1985).
- ²⁰G. F. V. Vort, *Metallography: Principle and Practice*; pp. 207-333, McGraw-Hill, New York, 1984.
- ²¹G. F. V. Vort and H. M. James, "Wrought Stainless Steels"; pp. 279-96 in *Metals Handbook*, Vol. 9, *Metallography and Microstructures*, Edited by K. Mills, J. R. Davis, J. D. Destefani, D. A. Dieferich, G. M. Crankovic, H. J. Frissel, and D. M. Jenkins. ASM International, Materials Park, OH, 1985.
- ²²J. D. Verhoeven, "Scanning Electron Microscopy"; pp. 490-515 in *Metals Handbook*, Vol. 10, *Materials Characterization*, Edited by K. Mills, J. R. Davis, J. D. Destefani, D. A. Dieferich, G. M. Crankovic, H. J. Frissel, and D. M. Jenkins. ASM International, Materials Park, OH, 1985.
- ²³R. Ruh, A. Zangvil, and J. Barlowe, "Elastic Properties of SiC, AlN, and Their Solid Solutions and Particulate Composites," *Am. Ceram. Soc. Bull.*, **64** [10] 1368-73 (1985).
- ²⁴R. N. Katz, S. Grendahl, K. Cho, I. Bar-On, and W. Rafaniello, "Fracture Toughness of Ceramics in the AlN-SiC System," *Ceram. Eng. Sci. Proc.*, **15** [3-4] 877-84 (1994).
- ²⁵A. Zangvil and R. Ruh, "Phase Relationships in the Silicon Carbide-Aluminum Nitride System," *J. Am. Ceram. Soc.*, **71** [10] 884-90 (1988).
- ²⁶H. A. Toutanji, D. Friel, T. El-Korchi, R. N. Katz, G. Wechsler, and W. Rafaniello, "Room Temperature Tensile and Flexural Strength of Ceramics in the AlN-SiC System," *J. Eur. Ceram. Soc.*, **15**, 425-34 (1995).
- ²⁷J.-F. Li and R. Watanabe, "Preparation and Mechanical Properties of SiC-AIN Ceramic Alloy," *J. Mater. Sci.*, **26** [17] 4813-17 (1991).
- ²⁸J. L. Huang and J. M. Jih, "Investigation of SiC-AIN System: Part II. Mechanical Properties," *J. Am. Ceram. Soc.*, **79** [5] 1262-64 (1996).
- ²⁹J. L. Huang and J. M. Jih, "Investigation of SiC-AIN System: Part I. Microstructure and Solid Solution," *J. Mater. Res.*, **10** [3] 651-57 (1995).
- ³⁰R.-R. Lee and W.-C. Wei, "Fabrication, Microstructure, and Properties of SiC-AIN Ceramic Alloys," *Ceram. Eng. Sci. Proc.*, **11** [7-8] 1094-121 (1990). □